IEEE Access
Multidisciplinary : Rapid Review : Open Access Journal

Received June 4, 2019, accepted June 15, 2019, date of publication June 24, 2019, date of current version July 16, 2019.

Digital Object Identifier 10.1109/ACCESS.2019.2924517

Prediction-Based Adaptive Sliding Mode Control for Remotely Piloted System With Time Delay and Parameter Uncertainty

HONGYANG XU, YONGHUA FAN, QUANCHENG LI, FAN WANG, AND JIE YAN
School of Astronautics, Northwestern Polytechnical University, Xi'an 710072, China
Corresponding author: Yonghua Fan (fyhlixin@163.com)

ABSTRACT This paper proposes a state prediction adaptive sliding mode (SPASM) control method for the remotely piloted system (RPS). With consideration of the time delay caused by the large transmission delay existing in the RPS, a prediction algorithm is proposed to provide the state prediction by using the state transition matrix. To approximate the uncertain lag of the remotely piloted vehicle (RPV) control augmentation system, an adaptive law is proposed to estimate the parameter uncertainties, and the overestimating problem is resolved efficiently. Meanwhile, to deal with the unmodeled dynamics and the predicted errors, a sliding mode controller is designed to guarantee the robustness of the whole closed-loop system. The simulation results show that the SPASM controller can not only guarantee the stability of the RPS in the presence of large time delay but also has a desirable performance of tracking the pilot's inputs while existing the unmodeled dynamics and parameter uncertainties.

INDEX TERMS Remotely piloted system (RPS), remotely piloted vehicle (RPV), time delay, state prediction, adaptive sliding mode control.

I. INTRODUCTION

Manned/unmanned aerial vehicle cooperative combat can simultaneously take advantages of manned vehicle with abilities of good battlefield perception and strong decision-making and the advantages of unmanned vehicle with abilities of flexible tactical maneuver, strongly sustained warfare ability and low cost. It can also effectively reduce casualties, thereby it will be an important mode of aerial combat in the future [1], [2]. The core problem of manned/unmanned aerial vehicle cooperative combat is to realize real-time remotely piloting of UAV [3], [4]. This kind of real-time remotely piloting is quite different from the current reconnaissance aircrafts, such as the Global Hawk and the Predator. Although these aircrafts have the function of remote control by the ground control station (GCS), the mission of the GCS is mostly limited to the UAV route command planning and target indication confirmation, instead of directly "piloting" the UAV in real time [5]–[7]. Therefore, in this control mode, time delay will only cause tracking deviation, and will not cause the instability of aircraft. However, a remotely piloted vehicle (RPV) should be "piloted" by a pilot in real time, ensuring that it can perform its various tactical missions.

In the remotely piloted mode, a pilot is away from the cockpit of a vehicle and its associated in-flight environment, he "pilots" the RPV through the over-the-horizon (OTH) data link and the pilot/vehicle interface display. However, because of the large transmission delay in the OTH data link, and the time delay is in the large loop in which pilot generates the inputs, the large transmission delay may cause the pilot to over-operate the RPV and even lead to RPV instability [8], [9]. Moreover, due to the strong maneuverability of RPV, its aerodynamic characteristics are very complex, and the coupling between aerodynamic parameters and flight dynamics are strong. In addition, unmodeled dynamics and parameter uncertainties always exist in large flight envelope and supersonic flight. These problems make it difficult to design the remotely piloted system (RPS). Therefore, it will be the vital technology for future manned/unmanned aerial vehicle cooperative combat under the conditions of large time delay, strong coupling, unmodeled dynamics and

The associate editor coordinating the review of this manuscript and approving it for publication was Ting Wang.

parameter uncertainties, ensuring the stability control of the RPS.

Over the past decades, the robust control of time delay systems and uncertain systems have been widely investigated, and many researches have been studied in this field, including predictive control [10]–[14], networked control [15]–[17], robust sliding mode control [18]–[20], adaptive control [21]–[23], and intelligent control [24]–[28]. In [29], an alternate approach to adapt the predictor model in real time using online parameter estimation techniques is developed to guarantee the tracking performance for a RPV. In [30], a novel predictor-based model reference adaptive controller is proposed to compensate for input delays in uncertain nonlinear systems, and the controller can guarantee that the estimation error decreases asymptotically to zero. Anouar Benamor [31] focuses on the robust adaptive sliding mode control law for uncertain discrete systems with unknown time-varying delay input, where the uncertainty is assumed unknown, and then, a new sliding mode surface is derived within the linear matrix inequalities. In [32], a control scheme combining the radial basis function neural network and discrete sliding mode control method is proposed for robust tracking and model following of uncertain time-delay systems with input nonlinearity. The proposed robust tracking controller guarantees the stability of an overall closed-loop system and achieves zero tracking error in the presence of input nonlinearity, time-delays, time-varying parameter uncertainties, and external disturbances. Zhang et al. [33] proposes a sliding mode predictive controller with a new robust global sliding mode surface for a certain networked control system with random time delay, mismatched parametric uncertainty, and external disturbances. Robust control for time-delay systems have been studied in many papers, however, most of them are concentrated on the input time delay system [30], [31], [33]–[35], others investigate the state time delay system, but the time delay system is mostly treated as an additional uncertain disturbance [32], [36], [37]. However, for the RPS, the state feedback of RPV in the overall closed loop is a pure time delay term, which should not be regarded as a simple uncertain disturbance.

To deal with the pure time delay system with state feedback, literatures [38] and [39] analyze the influence of the data link delay on the handling qualities of remotely piloted UAV, and a model-based predictor algorithm is used to improve UAV handling qualities by providing a ‘‘quickened display’’ to help the pilot compensate for its increased system time delay. The predictive display is found to substantially decrease pilot workload and improve Cooper-Harper ratings. However, due to unmodeled dynamics and parameter uncertainties of UAV, it will not have desirable tracking performance that the pilot's stick inputs are sent to the actuator of UAV directly. Therefore, in this paper we propose an innovative strategy of pilot/vehicle closed-loop system for RPS. The pilot's stick inputs are not sent to the RPV directly, instead the pilot's inputs are sent to the controller of RPS to calculate the remotely piloted commands, and then the commands as the reference signals are sent to the control augmentation system of RPV to realize the remote pilot of RPV in real time. It is well known that the adaptive sliding mode control (SMC) has its attractive features for the unmodeled dynamics and parameter uncertainties system [40]–[42]. In [43], two adaptive integral terminal sliding mode control schemes, namely, adaptive integral terminal sliding mode control scheme and adaptive fast integral terminal sliding mode control scheme are proposed for unmanned underwater vehicles to achieve the trajectory tracking control in the presence of dynamic uncertainties and time-varying external disturbance. In [44], an adaptive second-order fast nonsingular terminal sliding mode control scheme is proposed for the trajectory tracking of fully actuated autonomous underwater vehicles in the presence of dynamic uncertainties and time-varying external disturbances. The controller offers a faster convergence rate for the trajectory tracking control of fully actuated autonomous underwater vehicles.

In this paper, considering the RPS with large transmission delay, unmodeled dynamics and parameter uncertainties, a state prediction adaptive sliding mode (SPASM) controller of RPS is proposed. The main contributions of this paper are as follows:

1) An innovative strategy of pilot/vehicle closed-loop system is presented for RPS. The pilot's stick inputs are not sent to the actuator of RPV directly, instead the pilot inputs are sent to the controller of RPS to calculate the remotely piloted commands, and then the commands as the reference signals are sent to the control augmentation system of RPV to realize the remote pilot of RPV in real time.

2) A state predicted method based on sate transition matrix is proposed to remove the effects of transmission delay. The algorithm predicts the vehicle's final sate based on the remotely piloted command of RPS and current state of RPV. The predicted state is not only feedback to the controller, but also as a compensation providing a ‘‘quickened display’’ for pilot, which will help the pilot to rapidly see the effect of his inputs and determine next inputs.

3) The controller of the RPS is designed based on adaptive sliding mode control to guarantee the robustness of system considering the unmodeled dynamics and parameter uncertainties.

4) In this paper the main time delay of RPS is the transmission delay of data link, and once the bandwidth and the effective range of data link are selected, the time delay of transmission is known, nevertheless the lag caused by the control augmentation system of RPV is uncertain. Thereby the time delay in this paper is divided two parts: data link transmission delay is known, and the lag of the control augmentation system of RPV is unknown. The estimation of adaptive parameter is used to solve the delay deviation caused by the lag of RPV control augmentation system, and the sliding mode controller is used to solve the predicted errors caused by delay deviation of data link, which have ensured the stability of the whole closed-loop system.

The rest of this paper is organized as follows. The dynamics model of RPV and the composition of the RPS are formulated in Section II. An adaptive sliding mode controller based on state delay prediction is presented in Section III and its stability is also analyzed later. Section IV gives simulation results and some discussions. Finally, conclusions are given in Section V.

II. MODEL DESCRIPTION AND PROBLEM FORMULATION

A. DYNAMICS MODEL OF RPV

The dynamics model of RPV is described by Newton's 2nd law [45]. The details are shown as follows:

$$\begin{aligned}
\dot{V} &= -\frac{1}{m}D - g\sin\theta + d_V \\
\dot{\alpha} &= -\frac{1}{mV}L + q + \frac{g}{V}\cos\theta + d_\alpha \\
\dot{\theta} &= \frac{1}{mV}L - \frac{g}{V}\cos\theta + d_\theta \\
\dot{q} &= \frac{M_{yy}}{I_{yy}} + d_q \\
n_y &= \frac{L}{mg} + d_{n_y}
\end{aligned} \tag{1}$$

where V, α, θ and q represent velocity, angle of attack, flight-path angle and pitch rate of the RPV, respectively, I_{yy} and m stand for the moment of inertia and the mass, g is the acceleration owing to gravity, M_{yy} denotes the pitching moment of RPV, and it conforms to the sign convention that a positive pitch fin deflection produces a negative moment, D and L indicate the drag and lift of the RPV, respectively. $d_i\left(i = V, \alpha, \theta, q, n_y\right)$ are unknown unmodeled dynamics. The approximations of D, L and M_{yy} are expressed as follows:

$$\begin{aligned}
q &= \frac{1}{2}\rho V^2 \\
L &= q\bar{S}C_L\left(\alpha, \delta_e, Ma\right) \\
D &= q\bar{S}C_D\left(\alpha, \delta_e, Ma\right) \\
M_{yy} &= q\bar{S}\bar{c}\left(C_{M_{yy},\alpha}\left(\alpha, \delta_e, Ma\right) + C_{M_{yy},\delta_e}\left(\delta_e\right)\right)
\end{aligned} \tag{2}$$

where $\bar{S}, \bar{c}$ denote reference area and reference length. With

$$\begin{aligned}
\rho &= \rho_0 \exp\left(\frac{-\left(H - H_0\right)}{H_s}\right) \\
C_D &= C_D^0 + C_D^\alpha \alpha + C_D^{\delta_e}\delta_e + C_D^{Ma} Ma + C_D^{Ma\cdot\alpha} Ma\cdot\alpha \\
&\quad + C_D^{Ma\cdot\delta_e} Ma\cdot\delta_e + C_D^{Ma^2} Ma^2 + \Delta_D \\
C_L &= C_L^0 + C_L^\alpha \alpha + C_L^{\delta_e}\delta_e + C_L^{Ma} Ma + C_L^{\alpha^2}\alpha^2 + C_L^{\alpha\cdot\delta_e}\alpha\cdot\delta_e \\
&\quad + C_L^{Ma\cdot\alpha} Ma\cdot\alpha + C_L^{Ma\cdot\delta_e} Ma\cdot\delta_e + \Delta_L \\
C_{M_{yy}} &= C_{M_{yy}}^0 + C_{M_{yy}}^\alpha \alpha + C_{M_{yy}}^{\delta_e}\delta_e + C_{M_{yy}}^{\alpha^2}\alpha^2 + C_{M_{yy}}^{\alpha\cdot\delta_e}\alpha\cdot\delta_e \\
&\quad + C_{M_{yy}}^{Ma\cdot\alpha} Ma\cdot\alpha + C_{M_{yy}}^{Ma\cdot\delta_e} Ma\cdot\delta_e + \Delta_{M_{yy}}
\end{aligned} \tag{3}$$

where Ma is Mach, H is the altitude of RPV, H_0 is nominal altitude for air density approximation, $1/H_s$ is the air density decay rate, C_D is the drag coefficient with $C_D^i\,(i = 0, \alpha, \delta_e, Ma)$ is coefficient of i to C_D, C_L is the lift coefficient with $C_L^i\,(i = 0, \alpha, \delta_e, Ma)$ is coefficient of i to C_L, $C_{M_{yy}}$ is the pitching moment coefficient with $C_{M_{yy}}^i\,(i = 0, \alpha, \delta_e, Ma)$ is coefficient of i to $C_{M_{yy}}$, $\Delta_i\left(i = D, L, M_{yy}\right)$ are unknown uncertainties of the aerodynamic coefficients.

Remark 1: In fact, it is difficult to develop an exact model for RPV, since we cannot reproduce the complex flight environment of RPV in a wind tunnel. The expressions of D, L, M_{yy} are built by curve fitting techniques, so the unmodeled dynamics d_i and uncertain parameters Δ_i are inevitable.

B. PROBLEM FORMULATION

In this paper the RPS is a pilot/vehicle closed-loop system which consists of the RPV with control augmentation system, data link and remotely piloted station. The procedure of RPS is as follows: Pilot in the remotely piloted station sends the real-time stick inputs to RPS according to the vehicle predicted state parameters and situations displayed on the interface through the downstream channel of data link. The controller of RPS in remotely piloted station calculates the remotely piloted command based on the predicted state parameters, and the remotely piloted command is sent to RPV through the upstream channel of data link. The RPV control augmentation system tracks the remotely piloted command rapidly and precisely and changes the states of RPV. The state parameters of RPV collected by airborne data acquisition system are sent to remotely pilot station through downstream channel of data link.

In RPS the pilot's inputs cannot be sent to the RPV directly even if the vehicle has closed-loop control augmentation system independently, because the response of control augmentation system is greatly variable with altitude and velocity of RPV. Thereby if the pilot's inputs are sent to RPV directly, the large transmission delay and the uncertainties of RPV's controller response will cause pilot-induce oscillation (PIO) and engender the phenomenon of "chasing-swing", which will increase the pilot's workload and degrade the pilot/vehicle system stability and tracking performance.

Therefore, we present a SPASM controller for the pilot/vehicle closed-loop system, and the structure can be seen in Fig.1. The SPASM controller of RPS is designed to guarantee the stability of pilot/vehicle closed-loop system with large time delay and achieve high performance to track the pilot's inputs.

The latency in pilot/vehicle closed-loop system of RPS is defined as the time elapsed from pilot's inputs until an expected state feedback displayed in the pilot/vehicle interface. According to the generation of time delay, it primarily includes three parts. Uplink time delay τ_{up} refers to the time from the pilot's input to the remotely piloted command received by the RPV control augmentation system. For the same reason, τ_{down} is the downlink time delay from the state feedback of RPV to the pilot/vehicle interface display, and they are determined by the bandwidth and the effective

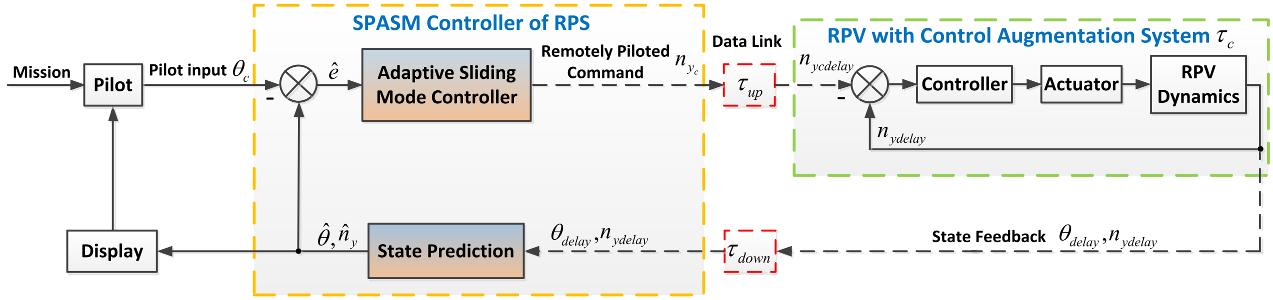

FIGURE 1. Principle of pilot/vehicle closed-loop system.

range of the data link. τ_c is the lag of the control augmentation system of RPV, which is variable with the altitude and velocity of vehicle. Therefore, in practical engineering, τ_{up}, and τ_{down} in RPS can be known in advance for a given data link, and the lag of the control augmentation system of RPV is unknown, thus the whole time delay in RPS is uncertain.

Remark 2: According to [33], the total time delay can be equivalent to the lag of the pilot/vehicle interface display. Therefore, the data link delay τ_{up} and τ_{down} can be combined into $\tilde{\tau}_d$ to make their analysis easier. Based on them, the time delay model is established as follows:

$$\tau_d = \tilde{\tau}_d + \tau_c \tag{4}$$

However, in the actual flight condition, the deviation of time delay is inevitable. In this paper, in order to ensure the stability of the whole closed-loop system, an adaptive law is used to solve the delay deviation caused by the lag of control system of RPV, and the sliding mode controller is used to solve the predicted errors caused by delay deviation of data link.

To achieve the closed-loop control of RPS, we need to choose an appropriate parameter as the remotely piloted command, which is used not only as the reference command of the RPV to perform tactical missions, but also as the control input of the RPS controller. Considering that the tactical maneuver is realized through the normal overload in combat, therefore, the normal overload command n_{yc} is used as the remotely piloted command of RPS. Moreover, the response characteristic of RPV control augmentation system needs to be considered because it greatly influences the stability of RPS. In order to effectively analyze and solve the influence of time delay on the stability of the RPS, the control augmentation system of RPV can be approximated as a first order model. However, because the characteristics of RPV controller are variable with altitude and velocity, the control augmentation system of RPV cannot be accurately modeled. Therefore, its time constant is time-varying and uncertain along with changes in flight environment. The approximately equivalent control augmentation system of RPV from the remotely piloted command n_{yc} to the output n_y is modeled as follows:

$$\dot{n}_y = \frac{1}{T(t)}\left(n_{yc} - n_y\right) \tag{5}$$

where $T(t)$ is a time-varying uncertain parameter, which is variable with altitude and velocity and denotes the lag of the control augmentation system of RPV τ_c.

According to the flight mission of RPV, the state space of RPS control augmentation system can be described as follows:

$$\begin{aligned} \dot{x}_1(t) &= A_{11}(t)\, x_1(t) + A_{12}(t)\, x_2(t) + \tilde{\Delta}_1 \\ \dot{x}_2(t) &= A_{22}(t)\, x_2(t) + B_2(t)\, u(t) + \tilde{\Delta}_2 \end{aligned} \tag{6}$$

where $x = \begin{bmatrix} x_1 & x_2 \end{bmatrix}^T = \begin{bmatrix} \theta & n_y \end{bmatrix}^T$ is the state vector, which full state is available for feedback, $u = n_{yc}$ is control input of the state space, it is also sent to RPV as remotely piloted command. The coefficient matrixes of the close loop system are as follows:

$$A(t) = \begin{bmatrix} A_{11} & A_{12} \\ A_{21} & A_{22} \end{bmatrix} = \begin{bmatrix} \dfrac{g\sin\theta}{V} & \dfrac{g}{V} \\ 0 & -\dfrac{1}{T(t)} \end{bmatrix},$$

$$B(t) = \begin{bmatrix} B_1 \\ B_2 \end{bmatrix} = \begin{bmatrix} 0 \\ \dfrac{1}{T(t)} \end{bmatrix}$$

with $\tilde{\Delta}_i\,(i = 1, 2)$ are the equivalent unknown factors, which represent not only parameter uncertainties and unmodeled dynamics, but also unknown nonlinear dynamics, nonlinear coupling and external disturbances [46].

Remark 3: In the affine model (6), we use $\tilde{\Delta}_i$ to represent the equivalent parameter uncertainties and unmodeled dynamics instead of a detailed expression of them. Derived from the unmodeled dynamics d_i in (1) and uncertain parameters Δ_i in (3), $\tilde{\Delta}_i$ is viewed as the congregational total of parameter uncertainties and unmodeled dynamics, and will be dealt with as a whole in this paper. Therefore, here we do not give the detailed expressions of $\tilde{\Delta}_i$. Similarly, we also do not give the detailed expressions of $\hat{\Delta}_i$ in (13).

Remark 4: Actually, the equivalent disturbances $\tilde{\Delta}_i$ are in existence of almost every equation, and obviously, they are hard to be modeled and measured. Unfortunately, they are actually in existence in the dynamics of RPV, so a robust controller against the equivalent disturbances is needed.

III. STATE PREDICTION BASED ADAPTIVE SLIDING MODE CONTROLLER DESIGN

A. STATE PREDICTION ALGORITHM

The algorithm is based on small perturbations linearized about an equilibrium state $\left(\theta_0\ n_{y0}\right)$, so we assume that all the unmodeled dynamics and parameter uncertainties do not exist. This means that $\tilde{\Delta}_i = 0$ in (6). Using delayed state parameters of RPV, small perturbations linearized aerodynamic model, and knowledge of the amount of time delay present, the algorithm predicts the future state of RPV based on remotely piloted command and current state. With the coefficient frozen method, the longitudinal dynamics (6) can be linearized as follows:

$$\begin{aligned} \dot{x}_1(t) &= A_{11}(t)\, x_1(t) + A_{12}(t)\, x_2(t) \\ \dot{x}_2(t) &= \bar{A}_{22}(t)\, x_2(t) + \bar{B}_2(t)\, u(t) \end{aligned} \tag{7}$$

where

$$\bar{A}(t) = \begin{bmatrix} A_{11} & A_{12} \\ A_{11} & \bar{A}_{22} \end{bmatrix} = \begin{bmatrix} \dfrac{g\sin\theta_0}{V} & \dfrac{g}{V} \\ 0 & -\dfrac{1}{\bar{T}} \end{bmatrix},$$

$$\bar{B}(t) = \begin{bmatrix} B_1 \\ \bar{B}_2 \end{bmatrix} = \begin{bmatrix} 0 \\ \frac{1}{\bar{T}} \end{bmatrix}$$

where $\bar{T}$ is a fixed value of the equivalent time constant about the equilibrium state $\left(\theta_0\ n_{y0}\right)$.

The RPV flight state is $x\left(t+\tilde{\tau}_d\right)$ at the flight time $\left(t+\tilde{\tau}_d\right)$, we assume that the data link delay time of RPS is $\tilde{\tau}_d$, then at the same time, the state feedback of RPV to the pilot/vehicle interface display is $x(t)$. Therefore, it is necessary to predict the state to ensure that the state feedback of RPV received by a pilot is synchronized with its real flight state. The solution for time-varying linear system is expressed as follows:

$$x(t) = \phi(t, t_0)\, x(t_0) + \int_{t_0}^{t} \phi(t, \tau) \bar{B} u(\tau)\, d\tau \tag{8}$$

where $\phi(t, \tau) = e^{\bar{A}(t-\tau)}$ is the state transition matrix. It can be seen from the above expression that the flight state at any time can be obtained as long as the initial state of RPV and the remotely piloted command are known. If $[t, \tau]$ is chosen to be equal to the period of time delay $\tilde{\tau}_d$, then $x(t)$ will be the predicted state vector $\tilde{\tau}_d$ seconds into the future. Knowledge of future remotely piloted command $u(t)$ is required to calculate the convolution integral. However, if remotely piloted command is assumed to remain constant during the time delay interval, a closed form solution is possible. Assuming that the remotely piloted command during the time delay interval is constant, the convolution integral in (8) may be written as follows:

$$\hat{x}(t) = \phi(t, t_0)\, x(t_0) + \left(\int_{t_0}^{t} \phi(t, \tau) d\tau\right) \bar{B} u(t_0) \tag{9}$$

Thus, the predicted state vector at time $t = \left(t_0 + \tilde{\tau}_d\right)$ is calculated with:

$$\begin{aligned} \hat{x}\left(t_0+\tilde{\tau}_d\right) &= \phi\left(t_0+\tilde{\tau}_d, t_0\right) x(t_0) \\ &\quad + \left(\int_{t_0}^{t_0+\tilde{\tau}_d} \phi\left(t_0+\tilde{\tau}_d, \tau\right) d\tau\right) \bar{B} u(t_0) \\ &= e^{\bar{A}\tilde{\tau}_d} x(t_0) + \left(\bar{A}^{-1} \cdot \left(e^{\bar{A}\tilde{\tau}_d} - I\right)\right) \bar{B} u(t_0) \end{aligned} \tag{10}$$

Substituting $\Phi = e^{\bar{A}\tilde{\tau}_d}$ and $\Theta = \bar{A}^{-1} \cdot \left(e^{\bar{A}\tilde{\tau}_d} - I\right)$, then the predicted state vector of RPV can be rewritten as:

$$\hat{x}\left(t_0+\tilde{\tau}_d\right) = \Phi x(t_0) + \Theta \bar{B} u(t_0) \tag{11}$$

According to the prediction algorithm in (11), we can obtain the state prediction of (7) as:

$$\begin{bmatrix} \hat{\theta}\left(t+\tilde{\tau}_d\right) \\ \hat{n}_y\left(t+\tilde{\tau}_d\right) \end{bmatrix} = \Phi \begin{bmatrix} \theta(t) \\ n_y(t) \end{bmatrix} + \Theta \bar{B} n_{yc}(t) \tag{12}$$

where $\hat{\theta}\left(t+\tilde{\tau}_d\right)$ and $\hat{n}_y\left(t+\tilde{\tau}_d\right)$ are the predicted values obtained with the state prediction algorithm at the flight time $\left(t+\tilde{\tau}_d\right)$.

B. DESIGN OF ADAPTIVE SLIDING MODE CONTROLLER

Considering the unmodeled dynamics and parameter uncertainties of (6), simultaneous equations (6) and (12), the RPV state space based on state prediction at the flight time $\left(t+\tilde{\tau}_d\right)$ can written as:

$$\begin{aligned} &\dot{\hat{x}}_1\left(t+\tilde{\tau}_d\right) \\ &= A_{11}\left(\Phi_{11}x_1(t) + \Phi_{12}x_2(t) + \Theta_1 B_1 u(t)\right) \\ &\quad + A_{12}\left(\Phi_{21}x_1(t) + \Phi_{22}x_2(t) + \Theta_2 \bar{B}_2 u(t)\right) + \hat{\Delta}_1 \\ &\quad \dot{\hat{x}}_2\left(t+\tilde{\tau}_d\right) = -\frac{1}{T}\left(\Phi_{21}x_1(t) + \Phi_{22}x_2(t) + \Theta_2 \bar{B}_2 u(t)\right) \\ &\quad + \frac{1}{T} u\left(t+\tilde{\tau}_d\right) + \hat{\Delta}_2 \end{aligned} \tag{13}$$

Remark 5: Because the state prediction algorithm is derived from the hypothesis that the small perturbation is linearized, predicted errors are inevitable. Thus, in the affine model (13), we use $\hat{\Delta}_i$ to represent the equivalent parameter uncertainties, unmodeled dynamics and the predicted errors of state prediction instead of a detailed expression of them.

Assumption 1: The given reference trajectory θ_c and corresponding derivative $\dot{\theta}_c$ are smooth and bounded.

Assumption 2: The equivalent disturbances $\hat{\Delta}_i$ are bounded as follows:

$$\begin{aligned} \left|\hat{\Delta}_1\right| &\le D_1 \\ \left|\hat{\Delta}_2\right| &\le D_2 \end{aligned}$$

The tracking error is defined as follows:

$$\hat{e} = \hat{x}_1 - x_c \tag{14}$$

where $x_c = \theta_c$ is the reference signal of RPV flight-path angle.

To design the sliding mode controller, the sliding mode surface is specified as:

$$s\left(\hat{x}\left(t+\tau_d\right)\right)=c\hat{e}\left(t+\tau_d\right)+\hat{x}_2\left(t+\tau_d\right) \tag{15}$$

where c is a positive constant. Taking the time derivative of sliding mode surface yields:

$$\begin{aligned}
&\dot{s}\left(\hat{x}\left(t+\tau_d\right)\right)\\
&\quad=c\dot{\hat{e}}\left(t+\tau_d\right)+c\dot{\hat{x}}_2\left(t+\tau_d\right)\\
&\quad=c\left(\dot{\hat{x}}_1\left(t+\tau_d\right)-\dot{x}_c\left(t+\tau_d\right)\right)+\dot{\hat{x}}_2\left(t+\tau_d\right)\\
&\quad=cA_{11}\left(\Phi_{11}x_1\left(t\right)+\Phi_{12}x_2\left(t\right)+\Theta_1B_1u\left(t\right)\right)\\
&\qquad+cA_{12}\left(\Phi_{21}x_1\left(t\right)+\Phi_{22}x_2\left(t\right)+\Theta_2\bar{B}_2u\left(t\right)\right)\\
&\qquad-c\dot{x}_c\left(t+\tau_d\right)-\frac{1}{T}\left(\Phi_{21}x_1\left(t\right)+\Phi_{22}x_2\left(t\right)\right)\\
&\qquad-\frac{1}{T}\Theta_2\bar{B}_2u\left(t\right)\ +\frac{1}{T}u\left(t+\tilde{\tau}_d\right)+c\hat{\Delta}_1+\hat{\Delta}_2
\end{aligned} \tag{16}$$

After designing the sliding mode surface, the next step is to design the sliding mode control law so that the reaching condition $s\left(\hat{x}\right)\dot{s}\left(\hat{x}\right)<0$ can be satisfied. This condition ensures that the control law will force the trajectories of the closed loop control system toward the sliding mode surface within finite time and all the trajectories will stay thereafter. To achieve the reaching condition, the control law is proposed as:

$$\begin{aligned}
u\left(t+\tilde{\tau}_d\right)=T&\left(-cA_{11}\left(\Phi_{11}x_1\left(t\right)+\Phi_{12}x_2\left(t\right)+\Theta_1B_1u\left(t\right)\right)\right.\\
&-cA_{12}\left(\Phi_{21}x_1\left(t\right)+\Phi_{22}x_2\left(t\right)+\Theta_2\bar{B}_2u\left(t\right)\right)\\
&+\frac{1}{T}\left(\Phi_{21}x_1\left(t\right)+\Phi_{22}x_2\left(t\right)+\Theta_2\bar{B}_2u\left(t\right)\right)\\
&\left.+c\dot{x}_c\left(t+\tau_d\right)-\eta\operatorname{sgn}\left(s\right)-k_ss\right)
\end{aligned} \tag{17}$$

where $\eta>cD_1+D_2$, k_s is a positive constant.

Lemma 1: With assumptions 1 and 2, if the control law (17) is applied, then the reaching condition is guaranteed.

Proof: Defining the following Lyapunov function:

$$V_1\left(\hat{x}\left(t+\tilde{\tau}_d\right)\right)=\frac{1}{2}s^T\left(\hat{x}\left(t+\tilde{\tau}_d\right)\right)s\left(\hat{x}\left(t+\tilde{\tau}_d\right)\right) \tag{18}$$

Then taking the derivative of V_1 and using (15) and (16), we have:

$$\begin{aligned}
&\dot{V}_1\left(\hat{x}\left(t+\tilde{\tau}_d\right)\right)\\
&\quad=s\left(\hat{x}\left(t+\tilde{\tau}_d\right)\right)\dot{s}\left(\hat{x}\left(t+\tilde{\tau}_d\right)\right)\\
&\quad=s\left(\hat{x}\left(t+\tilde{\tau}_d\right)\right)\left(cA_{11}\ \left(\Phi_{11}x_1\left(t\right)+\Phi_{12}x_2\left(t\right)\right)\right.\\
&\qquad+cA_{11}\Theta_1B_1u\left(t\right)+cA_{12}\left(\Phi_{21}x_1\left(t\right)+\Phi_{22}x_2\left(t\right)\right)\\
&\qquad+cA_{12}\Theta_2\bar{B}_2u\left(t\right)-c\dot{x}_c\left(t+\tau_d\right)-\frac{1}{T}\Phi_{21}x_1\left(t\right)\\
&\qquad-\frac{1}{T}\left(\Phi_{22}x_2\left(t\right)+\Theta_2\bar{B}_2u\left(t\right)\right)+\frac{1}{T}u\left(t+\tilde{\tau}_d\right)\\
&\qquad\left.+c\hat{\Delta}_1+\hat{\Delta}_2\right)
\end{aligned} \tag{19}$$

Then substituting $u\left(t+\tilde{\tau}_d\right)$ into (19) yields:

$$\begin{aligned}
\dot{V}_1=\ &s\left(c\,A_{11}\left(\Phi_{11}x_1\left(t\right)+\Phi_{12}x_2\left(t\right)+\Theta_1B_1u\left(t\right)\right)\right.\\
&+cA_{12}\left(\Phi_{21}x_1\left(t\right)+\Phi_{22}x_2\left(t\right)+\Theta_2\bar{B}_2u\left(t\right)\right)\\
&-c\dot{x}_c\left(t+\tau_d\right)-\frac{1}{T}\left(\Phi_{21}x_1\left(t\right)+\Phi_{22}x_2\left(t\right)+\Theta_2\bar{B}_2u\left(t\right)\right)\\
&-cA_{11}\left(\Phi_{11}x_1\left(t\right)+\Phi_{12}x_2\left(t\right)+\Theta_1B_1u\left(t\right)\right)\\
&-cA_{12}\left(\Phi_{21}x_1\left(t\right)+\Phi_{22}x_2\left(t\right)+\Theta_2\bar{B}_2u\left(t\right)\right)\\
&+\frac{1}{T}\left(\Phi_{21}x_1\left(t\right)+\Phi_{22}x_2\left(t\right)+\Theta_2\bar{B}_2u\left(t\right)\right)\\
&\left.+c\dot{x}_c\left(t+\tau_d\right)-\eta\operatorname{sgn}\left(s\right)-k_ss+c\hat{\Delta}_1+\hat{\Delta}_2\right)\\
=\ &-k_ss^2-\eta\left|s\right|+\left(c\hat{\Delta}_1+\hat{\Delta}_2\right)\cdot s\\
\leq\ &-k_ss^2\leq 0
\end{aligned} \tag{20}$$

The proof is completed.

Because T is an uncertain parameter, to estimate it, the adaptive sliding mode control law is designed. Let $\lambda=T$, then (13) can be rewritten as:

$$\begin{aligned}
\dot{\hat{x}}_1(t+\tilde{\tau}_d)&=A_{11}(\Phi_{11}x_1(t)+\Phi_{12}x_2(t)+\Theta_1B_1u(t))\\
&\qquad+A_{12}(\Phi_{21}x_1(t)+\Phi_{22}x_2(t)+\Theta_2\bar{B}_2u(t))+\hat{\Delta}_1\\
\lambda\dot{\hat{x}}_2(t+\tilde{\tau}_d)&=-(\Phi_{21}x_1(t)+\Phi_{22}x_2(t)+\Theta_2\bar{B}_2u(t))\\
&\qquad+u(t+\tilde{\tau}_d)+\hat{\Delta}_2
\end{aligned} \tag{21}$$

Assumption 3: Assuming the bound of the uncertain parameter λ as:

$$\lambda\in\Omega\left\{\lambda:0<\lambda_{\min}\leq\lambda\leq\lambda_{\max}\right\} \tag{22}$$

$\hat{\lambda}$ is defined as the estimated value of λ, the estimated error can be defined as:

$$\tilde{\lambda}=\hat{\lambda}-\lambda$$

The adaptive law of $\hat{\lambda}$ is

$$\dot{\hat{\lambda}}=-\cancel{\lambda}sc\Xi \tag{23}$$

where $\cancel{\lambda}>0$ and

$$\begin{aligned}
\Xi=\ &(-A_{11}(\Phi_{11}x_1(t)+\Phi_{12}x_2(t)+\Theta_1B_1u(t)).\\
&-A_{12}(\Phi_{21}x_1(t)+\Phi_{22}x_2(t)+\Theta_2\bar{B}_2u(t))+\dot{x}_c(t+\tau_d)
\end{aligned}$$

Then the SPASM controller can be obtained as:

$$\begin{aligned}
u^*\left(t+\tilde{\tau}_d\right)=&-\hat{\lambda}cA_{11}\left(\Phi_{11}x_1\left(t\right)+\Phi_{12}x_2\left(t\right)+\Theta_1B_1u\left(t\right)\right)\\
&-\hat{\lambda}cA_{12}\left(\Phi_{21}x_1\left(t\right)+\Phi_{22}x_2\left(t\right)+\Theta_2\bar{B}_2u\left(t\right)\right)\\
&+\left(\Phi_{21}x_1\left(t\right)+\Phi_{22}x_2\left(t\right)+\Theta_2\bar{B}_2u\left(t\right)\right)\\
&+\hat{\lambda}c\dot{x}_c\left(t+\tau_d\right)-\eta\operatorname{sgn}\left(s\right)-k_ss
\end{aligned} \tag{24}$$

Lemma 2: With assumptions 1-3, if the control law (24) is applied, then the reaching condition is guaranteed.

Proof: Defining the following Lyapunov function

$$V_2\left(\hat{x}\left(t+\tilde{\tau}_d\right)\right)=\frac{1}{2}\lambda s^T\left(\hat{x}\left(t+\tilde{\tau}_d\right)\right)s\left(\hat{x}\left(t+\tilde{\tau}_d\right)\right)+\frac{1}{2\cancel{\lambda}}\tilde{\lambda}^2 \tag{25}$$

Then taking the derivative of V_2, we have:

$$\begin{aligned}
&\dot{V}_2\left(\hat{x}\left(t+\tilde{\tau}_d\right)\right)\\
&\quad=\lambda s\left(\hat{x}\left(t+\tilde{\tau}_d\right)\right)\dot{s}\left(\hat{x}\left(t+\tilde{\tau}_d\right)\right)+\frac{1}{\cancel{\lambda}}\tilde{\lambda}\dot{\hat{\lambda}}
\end{aligned}$$

$$\begin{aligned}
&= s\left(\hat{x}\left(t+\tilde{\tau}_d\right)\right)\left(\lambda c A_{11}\left(\Phi_{11}x_1(t)+\Phi_{12}x_2(t)\right)\right.\\
&\quad +\lambda c A_{11}\Theta_1 B_1 u(t)+\lambda c A_{12}\Phi_{21}x_1(t)\\
&\quad +\lambda c A_{12}\left(\Phi_{22}x_2(t)+\Theta_2\bar{B}_2 u(t)\right)\\
&\quad -\lambda c\dot{x}_c\left(t+\tau_d\right)-\left(\Phi_{21}x_1(t)+\Phi_{22}x_2(t)\right)\\
&\quad \left.+\Theta_2\bar{B}_2 u(t)+u^*\left(t+\tilde{\tau}_d\right)+c\hat{\Delta}_1+\hat{\Delta}_2\right)\\
&\quad +\frac{1}{\cancel{\lambda}}\tilde{\lambda}\left(-\cancel{\lambda} sc\Xi\right) \qquad (26)
\end{aligned}$$

Then substituting $u^*\left(t+\tilde{\tau}_d\right)$ into (26) yields:

$$\begin{aligned}
\dot{V}_2 &= s\left(\lambda c A_{11}\left(\Phi_{11}x_1(t)+\Phi_{12}x_2(t)+\Theta_1 B_1 u(t)\right)\right.\\
&\quad +\lambda c A_{12}\left(\Phi_{21}x_1(t)+\Phi_{22}x_2(t)+\Theta_2\bar{B}_2 u(t)\right)\\
&\quad -\lambda c\dot{x}_c\left(t+\tau_d\right)-\left(\Phi_{21}x_1(t)+\Phi_{22}x_2(t)+\Theta_2\bar{B}_2 u(t)\right)\\
&\quad -\hat{\lambda} c A_{11}\left(\Phi_{11}x_1(t)+\Phi_{12}x_2(t)+\Theta_1 B_1 u(t)\right)\\
&\quad -\hat{\lambda} c A_{12}\left(\Phi_{21}x_1(t)+\Phi_{22}x_2(t)+\Theta_2\bar{B}_2 u(t)\right)\\
&\quad +\left(\Phi_{21}x_1(t)+\Phi_{22}x_2(t)+\Theta_2\bar{B}_2 u(t)\right)\\
&\quad \left.+\hat{\lambda} c\dot{x}_c\left(t+\tau_d\right)-\eta\,\mathrm{sgn}(s)-k_s s+c\hat{\Delta}_1+\hat{\Delta}_2\right)\\
&\quad +\frac{1}{\cancel{\lambda}}\tilde{\lambda}\left(-\cancel{\lambda} sc\Xi\right) \qquad (27)
\end{aligned}$$

So

$$\begin{aligned}
\dot{V}_2 &= s\left(-\tilde{\lambda} c A_{11}\left(\Phi_{11}x_1(t)+\Phi_{12}x_2(t)+\Theta_1 B_1 u(t)\right)\right.\\
&\quad -\tilde{\lambda} c A_{12}\left(\Phi_{21}x_1(t)+\Phi_{22}x_2(t)+\Theta_2\bar{B}_2 u(t)\right)\\
&\quad \left.+\tilde{\lambda} c\dot{x}_c\left(t+\tau_d\right)-\eta\,\mathrm{sgn}(s)-k_s s+c\hat{\Delta}_1+\hat{\Delta}_2\right)\\
&\quad +\frac{1}{\cancel{\lambda}}\tilde{\lambda}\left(-\cancel{\lambda} sc\Xi\right)\\
&= -k_s s^2-\eta|s|+\left(c\Delta_1+\Delta_2\right)\cdot s\\
&\leq -k_s s^2 \qquad (28)
\end{aligned}$$

The proof is completed. According to the LaSalle invariance principle, the closed loop system is asymptotically stable. When $t\to\infty$, $s\to 0$ and $\tilde{\lambda}\to 0$, convergence rate depends on k_s.

To eliminate the chattering of adaptive sliding mode controller, we adopt hyperbolic tangent function instead of sign function. Then the control law (24) is modified to be:

$$\begin{aligned}
u^*\left(t+\tilde{\tau}_d\right) &= -\hat{\lambda} c A_{11}\left(\Phi_{11}x_1(t)+\Phi_{12}x_2(t)+\Theta_1 B_1 u(t)\right)\\
&\quad -\hat{\lambda} c A_{12}\left(\Phi_{21}x_1(t)+\Phi_{22}x_2(t)+\Theta_2\bar{B}_2 u(t)\right)\\
&\quad +\left(\Phi_{21}x_1(t)+\Phi_{22}x_2(t)+\Theta_2\bar{B}_2 u(t)\right)\\
&\quad +\hat{\lambda} c\dot{x}_c\left(t+\tau_d\right)-\eta\tanh\left(\varepsilon^{-1}s\right)-k_s s \qquad (29)
\end{aligned}$$

where $\varepsilon>0$ is a designed parameter. Then (28) can be rewritten as

$$\dot{V}_2 = -k_s s^2-\eta s\tanh\left(\varepsilon^{-1}s\right)+\left(c\Delta_1+\Delta_2\right)\cdot s \qquad (30)$$

lemma 3: For any $x\in R$ and any $\sigma>0$ the following inequality holds [47]:

$$0\leq |x|-\left|x\tanh\frac{x}{\sigma}\right|\leq \mu\sigma \qquad (31)$$

where μ is a constant that satisfies $\mu = e^{-(\mu+1)}$, so $\mu = 0.2785$. The proof of the above lemma follows after straightforward algebraic manipulation and is therefore omitted.

lemma 4: For any $V:[0,\infty)\in R$, the solution about inequality $\dot{V}\leq -\kappa V+f$, $\forall t\geq t_0\geq 0$ as follows [48]:

$$V(t)\leq e^{-\kappa(t-t_0)}V(t_0)+\int_{t_0}^{t}e^{-\kappa(t-\tau)}f(\tau)\,d\tau \qquad (32)$$

where κ is an arbitrary constant.

According to lemma 3, we have:

$$|s|-s\tanh\left(\varepsilon^{-1}s\right)\leq \mu\varepsilon \qquad (33)$$

Then $\eta|s|-\eta s\tanh\left(\varepsilon^{-1}s\right)\leq\eta\mu\varepsilon$, that is

$$-\eta s\tanh\left(\varepsilon^{-1}s\right)\leq -\eta|s|+\eta\mu\varepsilon \qquad (34)$$

So we can get

$$\begin{aligned}
\dot{V}_2 &\leq -k_s s^2-\eta|s|+\eta\mu\varepsilon+\left(c\Delta_1+\Delta_2\right)\cdot s\\
&\leq -k_s s^2+\eta\mu\varepsilon \qquad (35)
\end{aligned}$$

Let

$$-\cancel{k_s} s^2+\eta\mu\varepsilon=-\frac{2k_s}{\lambda}V_2+\frac{k_s}{\cancel{\lambda}\lambda}\tilde{\lambda}^2+\eta\mu\varepsilon=-\kappa V_2+f \qquad (36)$$

where $\kappa=\frac{2k_s}{\lambda}$, $f=\frac{k_s}{\cancel{\lambda}\lambda}\tilde{\lambda}^2+\eta\mu\varepsilon$.

According to lemma 4, the solution of inequality $\dot{V}_2\leq -\kappa V_2+f$ is

$$\begin{aligned}
V_2(t) &\leq e^{-\kappa(t-t_0)}V_2(t_0)+\int_{t_0}^{t}e^{-\kappa(t-\tau)}f(\tau)\,d\tau\\
&= e^{-\kappa(t-t_0)}V_2(t_0)+\frac{f}{\kappa}\left(1-e^{-2k_s(t-t_0)}\right) \qquad (37)
\end{aligned}$$

So

$$\lim_{t\to\infty}V_2(t)\leq\frac{f}{\kappa} \qquad (38)$$

Thus all the signals included in the Lyapunov function $V_2(t)$ are bounded [49].

Remark 6: In order to prevent the control input $u^*\left(t+\tilde{\tau}_d\right)$ excessive caused by overestimation problem of $\hat{\lambda}$, or $\hat{\lambda}\leq 0$, it is necessary to modify the adaptive law to limit $\hat{\lambda}$ within the range of $\left[\lambda_{\min}\ \lambda_{\max}\right]$, A mapping adaptive law can be used to modify (23)

$$\dot{\hat{\lambda}}=\mathrm{Proj}_{\hat{\lambda}}\left(-\cancel{\lambda} sc\Xi\right) \qquad (39)$$

where

$$\mathrm{Proj}_{\hat{\lambda}}(\cdot)=\begin{cases}0\ \mathit{if}\ \hat{\lambda}\geq\lambda_{\max}\ \text{and}\ \cdot>0\\ 0\ \mathit{if}\ \hat{\lambda}\leq\lambda_{\max}\ \text{and}\ \cdot 0\\ \text{otherwise}\end{cases} \qquad (40)$$

That is, when $\hat{\lambda}$ exceeds the maximum value, if there is a tendency to continue to increase, that is $\dot{\hat{\lambda}}>0$, then the value of $\hat{\lambda}$ remains unchanged. When $\hat{\lambda}$ exceeds the minimum value, if there is a tendency to continue to decrease, that is $\dot{\hat{\lambda}}<0$, then the value of $\hat{\lambda}$ remains unchanged.

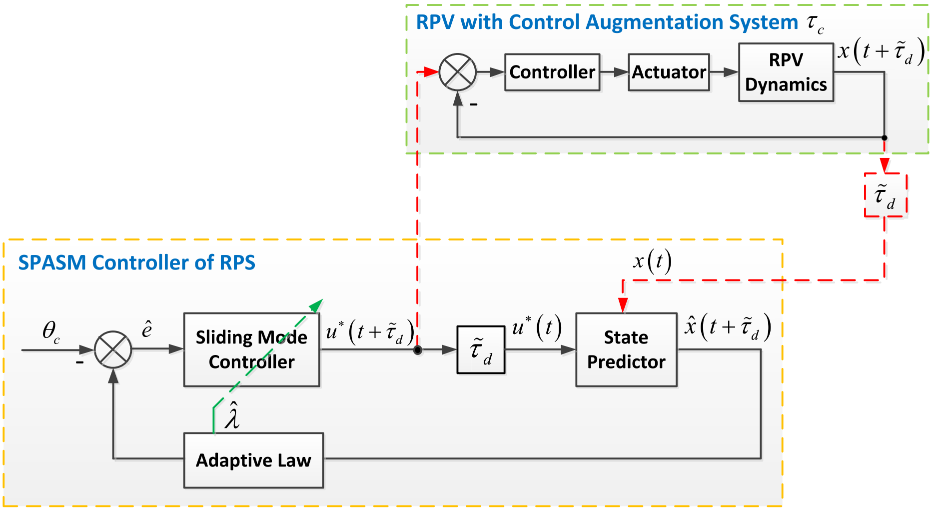

FIGURE 2. **The structure of SPASM controller for RPS.**

Remark 7: Using the modified adaptive law can guarantee $\tilde{\lambda}\left(\Xi + \frac{1}{\bar{\lambda}}\dot{\hat{\lambda}}\right) \leq 0$, thus asymptotical convergence of $V_2(t)$ is ensured.

Therefore, the structure of SPASM controller for RPS is shown as Fig. 2.

IV. SIMULATION

In this section, three numerical examples are given to illustrate the effectiveness and the robustness of the SPASM controller. The initial state variables are set as $H_0 = 8000m$, $V_0 = 246m/s$, $\alpha_0 = 0\,rad$, $\theta_0 = 0\,rad$, $q_0 = 0\,rad/s$, $n_{y0} = 0g$.

In this paper, assuming that a given control augmentation system of RPV is a typical three-loop controller. The control law is employed as follow:

$$\delta_e = k_q\left(k_\alpha\left(\int k_{n_y}\left(n_{yc} - n_{yRPV}\right)dt - \alpha\right) - q\right)$$

where k_{n_y}, k_α and k_q are the control gains, which are selected as $k_{n_y} = 0.15$, $k_\alpha = 4.1729$ and $k_q = -0.3738$, $e_{n_{yRPV}} = n_{yc} - n_{yRPV}$ is the tracking error of control augmentation system of RPV. According to the dynamic characteristics of the control augmentation system of RPV, we can approximate the equivalent time constant as $\bar{T} = 0.28$ sec.

The estimated parameter $\hat{\lambda}(t)$ is initialized at zero initial conditions. The proposed controller parameters are chosen as $\bar{\lambda} = 0.2$, $c = 15$, $\eta = 5$, $\varepsilon = 0.1$, $k_s = 0.5$, $\lambda_{\min} = 0.1$, $\lambda_{\max} = 0.4$.

To compare the advantages of the SPASM controller with those of the conventional LQR controller in the conditions of large time delay, unmodeled dynamics and parameter uncertainties, a LQR controller with similar dynamic characteristics is used.

Case I. $\tilde{\tau}_d = 0$, $\hat{\Delta}_i = 0$

To test the tracking performance of the proposed method, a step reference signal is utilized here. The step reference signal considered in this paper is $\theta_c = 0.35$ rad. With considering the overload of RPV, the step reference signal should pass a second-order prefilter to get a smooth trajectory. The prefilter is chosen as

$$\theta_{filter}(s) = \frac{\omega_n^2}{s^2 + 2\zeta\omega_n + \omega_n^2}$$

with $\zeta = 1$, $\omega_n = 0.928 rad/s$.

The tracking performances of the SPASM controller and LQR controller can be found in Fig. 3, where the solid line represents the given reference signal that needs to be tracked, the dash line represents the response of the LQR controller, and the dashdot line represents the response of the SPASM controller. In Fig. 3, we can see that both the LQR controller and the SPASM controller all have good tracking performances under the conditions of no time delay and no parameter uncertainties, and the tracking error are accepted small.

Case II. $\tilde{\tau}_d = 0.5$ sec, $\hat{\Delta}_i \neq 0$

In this numerical example, the unknown unmodeled dynamics of RPV, $d_i\left(i = V, \alpha, \theta, q, n_y\right)$, are considered in the simulations and take the following values:

$$\begin{aligned}
d_V &= 0.06\sin(0.5t)\\
d_\alpha &= 0.05\sin(0.2t)\\
d_\theta &= 0.0002\sin(0.4t)\\
d_\vartheta &= 0.005\sin(0.3t)\\
d_q &= 0.001\sin(0.6t)\\
d_{n_y} &= 0.003\sin(0.7t)
\end{aligned}$$

The uncertainties of the aerodynamic coefficients in (3), $\Delta_i\left(i = D, L, M_{yy}\right)$, are chosen as maximum 10%, 10% and 30% deviated from the nominal parameters respectively. The equivalent time delay is set to $\tilde{\tau}_d = 0.5s$, to examine the availability of proposed controller. From the Section III, we can

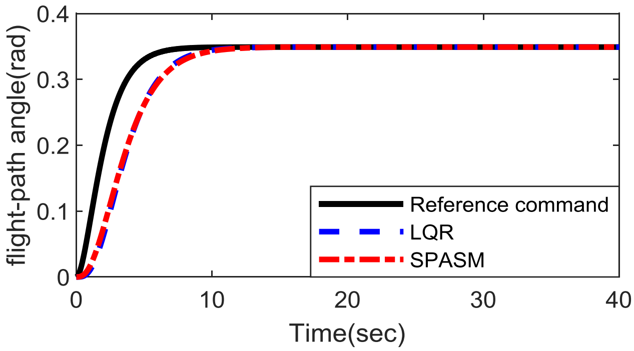

(a)

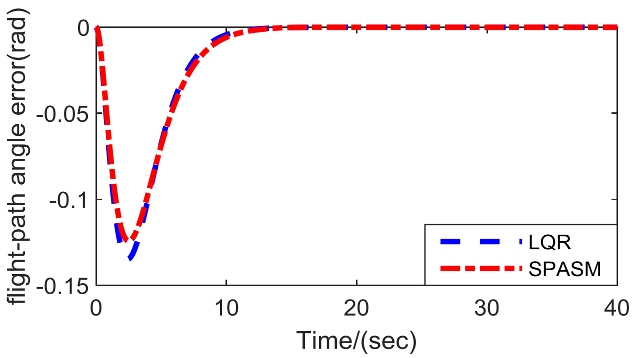

(b)

FIGURE 3. **Fight-path angle tracking.**

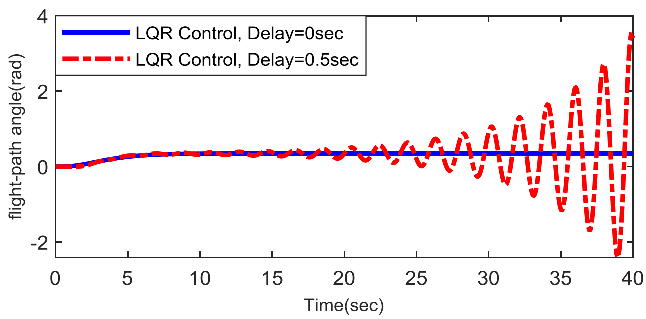

FIGURE 4. **LQR controller fight-path angle tracking with 0.5sec delay.**

calculate the state predictive parameters Φ and Θ as follows:

$$\Phi = \begin{bmatrix} 1 & 0.009 \\ 0 & 0.168 \end{bmatrix}, \Theta = \begin{bmatrix} 0.5 & 0.003 \\ 0 & 0.233 \end{bmatrix}$$

For comparison, we use the same reference signal with Case I, the tracking performance of LQR controller and SPASM controller can be found in Fig. 4 and Fig. 5, respectively. In Fig. 4, we can see that in the conditions of time delay, unmodeled dynamics and parameter uncertainties, the response of flight-path angle is oscillation and divergence, it means that the close-loop system is instability. From Fig. 5, we can see that although the simulation example has large time delay, unmoleded dynamics and parameter uncertainties, the SPASM controller can maintain desirable tracking of the reference signal.

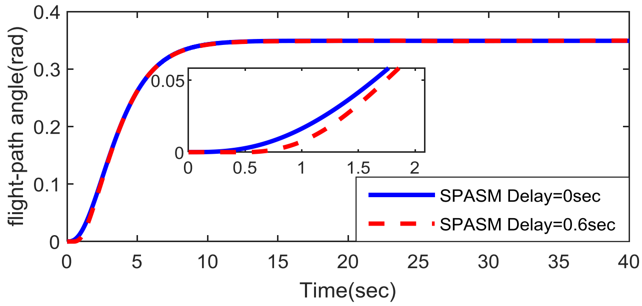

FIGURE 5. **SPASM controller fight-path angle tracking with 0.5sec delay.**

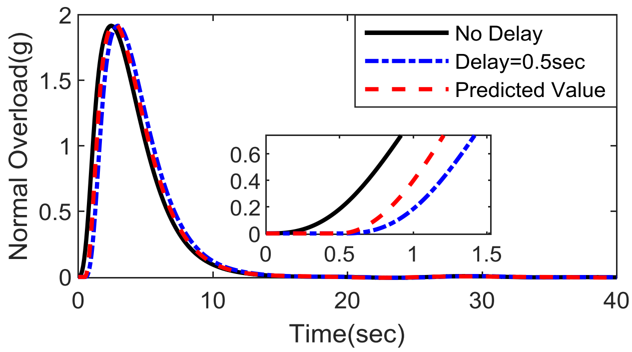

(a)

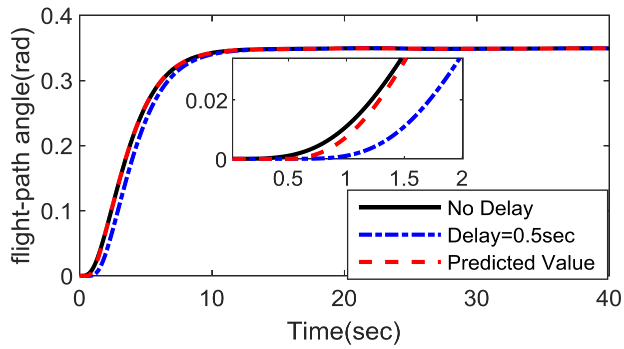

(b)

FIGURE 6. **SPASM controller state prediction with 0.5sec delay.**

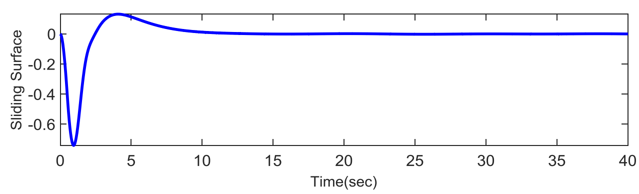

FIGURE 7. **SPASM controller sliding surface with 0.5sec delay.**

Fig. 6 shows the state predictive values of normal overload and flight-path angle, where the solid line represents the reference value with no time delay, the dashdot line represents the response of time delay $\tilde{\tau}_d = 0.5$ sec with no state prediction, and the dash line represents the predictive value of time delay $\tilde{\tau}_d = 0.5$ sec with state predictive method proposed in this paper. In Fig. 6, we can see that the predictive values can quickly track the reference value at simulation time 0.5 sec.

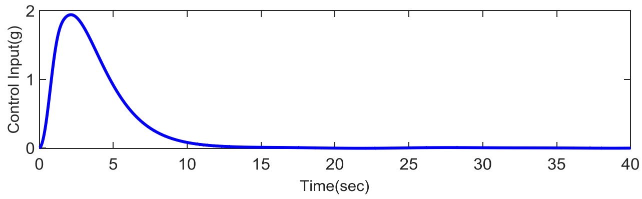

FIGURE 8. SPASM controller control input with 0.5sec delay.

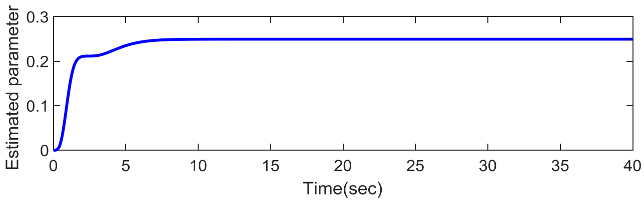

FIGURE 9. SPASM controller estimated parameter with 0.5sec delay.

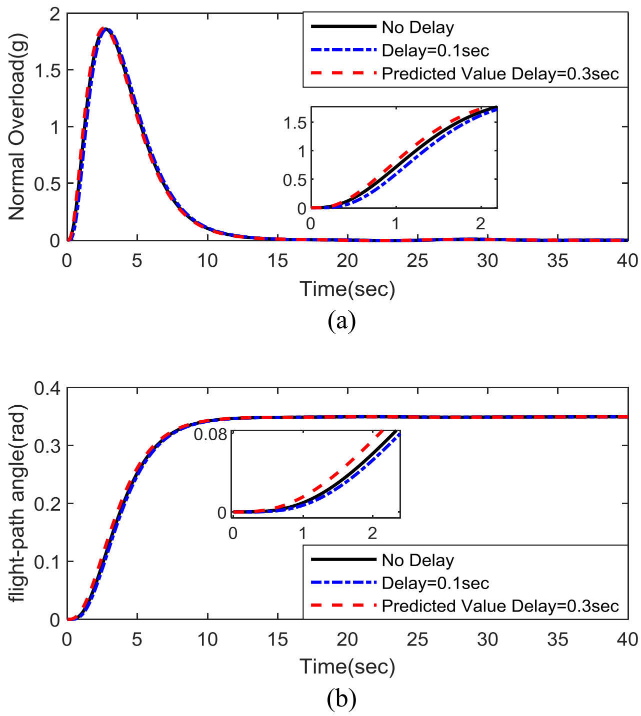

FIGURE 10. SPASM controller state prediction with $\tilde{\tau}_d - \Delta\tilde{\tau}_d$ delay.

The other control parameters are given in Fig. 7-Fig. 9. According the sliding surface and the control input shown in Fig.7 and Fig.8, we can see that the sliding surface and the control input are smooth and bounded. Fig. 9 shows the estimated parameter $\hat{\lambda}$ of the control augmentation system of RPV, and that the estimated parameter value converges to 0.25. Therefore the proposed SPASM controller can achieve good performance for the RPS with large time delay, unmoldeled dynamics and parameter uncertainties. From the simulation results, the validity of the proposed controller can be easily testified.

Case III. Validation of robustness

To demonstrate the robustness of the proposed method, ± 0.2 sec deviation of time delay is considered in case III. In this numerical example, the equivalent time delay is

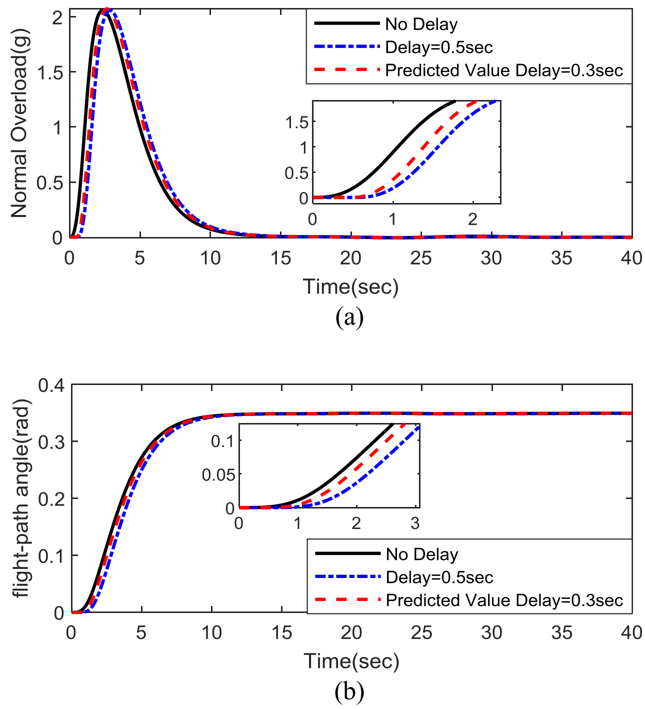

FIGURE 11. SPASM controller state prediction with $\tilde{\tau}_d + \Delta\tilde{\tau}_d$ delay.

set to $\tilde{\tau}_d = 0.3$ sec, the deviation of time delay is $\Delta\tilde{\tau}_d = 0.2s$, the unknown unmodeled dynamics of RPV, $d_i \left(i = V, \alpha, \theta, q, n_y\right)$ and the uncertainties of the aerodynamic coefficients in (3),$\Delta_i \left(i = D, L, M_{yy}\right)$, are same as case II. From the Section III, we can calculate the state predictive parameters Φ and Θ as follows:

$$\Phi = \begin{bmatrix} 1 & 0.007 \\ 0 & 0.343 \end{bmatrix}, \Theta = \begin{bmatrix} 0.3 & 0.001 \\ 0 & 0.184 \end{bmatrix}$$

For comparison, we use the same reference signal with Case I. Fig. 10 shows the state predictive values of normal overload and flight-path angle with time delay deviation of -0.2 sec, where the solid line represents the reference value with no time delay, the dashdot line represents the response of time delay $\tilde{\tau}_d - \Delta\tilde{\tau}_d = 0.1$ sec with no state prediction, and the dash line represents the predictive value of time delay $\tilde{\tau}_d = 0.3$ sec with state prediction method proposed in this paper. In Fig. 10, we can see that the predictive values can quickly track the reference value, but because of the time delay deviation of -0.2 sec, the predictive value will be slightly ahead of the reference value. Fig. 11 shows the state predictive values with time delay deviation of 0.2 sec, where the dashdot line represents the response of time delay $\tilde{\tau}_d + \Delta\tilde{\tau}_d = 0.5$ sec with no state prediction, and the dash line represents the predictive value of time delay $\tilde{\tau}_d = 0.3$ sec. In Fig. 11, we can see that the predictive values can quickly track the reference value, but because of the time delay deviation of 0.2 sec, the predictive value will lag slightly behind the reference value.

The control input and the tracking performance of SPASM controller can be found in Fig. 12 and Fig. 13 respectively

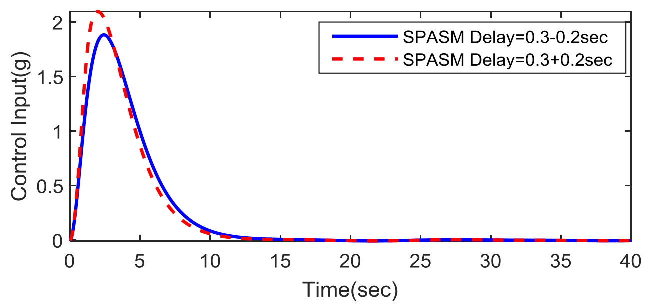

FIGURE 12. SPASM controller control input with $\tilde{\tau}_d \pm \Delta\tilde{\tau}_d$ delay.

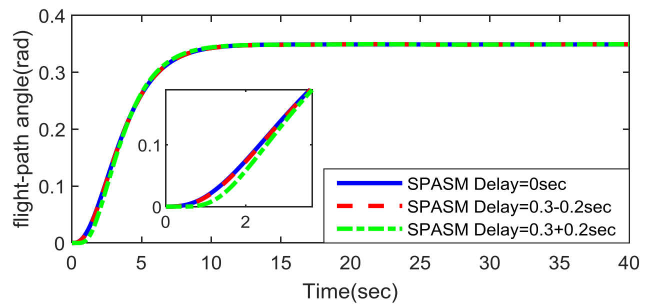

FIGURE 13. SPASM controller fight-path angle tracking with $\tilde{\tau}_d \pm \Delta\tilde{\tau}_d$ delay.

when the time delay is $\tilde{\tau}_d \pm \Delta\tilde{\tau}_d$. From Fig. 12, we can see that the control input is smooth and bounded. From Fig. 13, we can see that despite time delay deviation, unmoleded dynamics and parameter uncertainties existing in the simulation, the response curves are smooth and stable. Therefore, the proposed SPASM controller has sufficient robustness to maintain the desirable tracking performance.

V. CONCLUSIONS

In this paper, an innovative strategy of pilot/vehicle closed-loop system is presented and an adaptive sliding mode control method based on state delay prediction is designed for the RPS. With consideration of the time delay caused by the great transmission delay existing in RPS, a prediction algorithm is proposed to provide the state prediction by using the state transition matrix. To approximate the uncertain lag of RPV control augmentation system, an adaptive law is proposed to estimate the parameter uncertainties, and the overestimating problem is resolved efficiently. Meanwhile, to deal with the unmodeled dynamics and the predicted errors, a sliding mode controller is designed to guarantee the robustness of the whole closed-loop system. Simulation results show that the SPASM controller can not only guarantee the stability of RPS in the presence of large time delay, but also has desirable performance of tracking the pilot's inputs while existing unmodeled dynamics and parameter uncertainties.

REFERENCES

[1] Z. Yun, Y. Peiyang, Z. Jieyong, and W. Lujun, "Formation and adjustment of manned/unmanned combat aerial vehicle cooperative engagement system," *J. Syst. Eng. Electron.*, vol. 29, no. 4, pp. 756–767, Aug. 2018.
[2] Z. Shu, W. Wang, and R. Wang, "Design of an optimized architecture for manned and unmanned combat system-of-systems: Formulation and coevolutionary optimization," *IEEE Access*, vol. 6, pp. 52725–52740, 2018.
[3] J. Fan, D. Li, R. Li, T. Yang, and Q. Wang, "Analysis for cooperative combat system of manned-unmanned aerial vehicles and combat simulation," in *Proc. IEEE ICUS*, Oct. 2017, pp. 204–209.
[4] J. Chen, Q. Zhang, and B. Hou, "An assessment method of pilot workload in manned/unmanned-aerial-vehicles team," in *Proc. IEEE ICSPCC*, Oct. 2017, pp. 1–5.
[5] F. Schmitt and A. Schulte, "Mixed-initiative interaction in manned-unmanned-teaming mission planning: Design and evaluation of a prototype," in *Proc. AIAA SciTech Forum*, Kissimmee, FL, USA, Jan. 2015, p. 0114.
[6] N. S. Rader and M. L. Reagan, "Human-in-the-loop operations over time delay: Lessons learned," in *Proc. 43rd Int. Conf. Environ. Syst.*, 2013, p. 3520.
[7] D. Geister, G. Schwoch, and H. Becker, "Flight testing of optimal remotely-piloted-aircraft-system scan patterns," *J. Aircr.*, vol. 54, no. 5, pp. 1675–1691, Sep. 2017.
[8] A. Majka, "Remotely piloted aircraft system with optimum avoidance maneuvers," *J. Aerosp. Eng.*, vol. 232, no. 7, pp. 1247–1257, 2017.
[9] F. Wang, S. Qi, and L. Jing, "An analysis of time-delay for remote piloted vehicle," in *Proc. Int. Conf. Mech., Mater. Aerosp. Eng.*, Jul. 2017, pp. 1–6.
[10] V. L. Kharitonov, "Prediction-based control for systems with state and several input delays," *Automatica*, vol. 79, pp. 11–16, May 2017.
[11] R. Sanz, P. García, Q.-C. Zhong, and P. Albertos, "Predictor-based control of a class of time-delay systems and its application to quadrotors," *IEEE Trans. Ind. Electron.*, vol. 64, no. 1, pp. 459–469, Jan. 2017.
[12] J. S. Nandiganahalli, C. Kwon, and I. Hwang, "Prediction-based adaptive robust control for a class of uncertain time-delay systems," *IFAC-PapersOnLine*, vol. 50, no. 1, pp. 6489–6494, 2017.
[13] T. Fricke and F. Holzapfel, "An approach to flight control with large time delays derived from a pulsive human control strategy," in *Proc. AIAA SciTech Forum*, CA, USA, Jan. 2016, pp. 1–7.
[14] F. Zhang, T. Fricke, and F. Holzapfel, "Integrated control and display augmentation for manual remote flight control in the presence of large latency," in *Proc. AIAA SciTech Forum*, CA, USA, Jan. 2016, pp. 1–11.
[15] Z. Hui, Y. Shi, J. Wang, and H. Chen, "A new delay-compensation scheme for networked control systems in controller area networks," *IEEE Trans. Ind. Electron.*, vol. 65, no. 9, pp. 7239–7247, Sep. 2018.
[16] H. Lu, C. Guo, and Y. Hu, "Robust H_∞ control of lurie nonlinear stochastic network control systems with multiple additive time-varying delay components," *IEEE Access*, vol. 7, pp. 3390–3405, 2019.
[17] Y. Jiang, J. Fan, T. Chai, F. L. Lewis, and J. Li, "Tracking control for linear discrete-time networked control systems with unknown dynamics and dropout," *IEEE Trans. Neural Netw. Learn. Syst.*, vol. 29, no. 10, pp. 4607–4620, Oct. 2018.
[18] S. He, J. Song, and F. Liu, "Robust finite-time bounded controller design of time-delay conic nonlinear systems using sliding mode control strategy," *IEEE Trans. Syst., Man, Cybern., Syst.*, vol. 48, no. 11, pp. 1863–1873, Nov. 2018.
[19] F. Huang, W. Zhang, Z. Chen, J. Tang, W. Song, and S. Zhu, "RBFNN-based adaptive sliding mode control design for nonlinear bilateral teleoperation system under time-varying delays," *IEEE Access*, vol. 7, pp. 11905–11912, 2019.
[20] R. Liu, X. Cao, and M. Liu, "Finite-time synchronization control of spacecraft formation with network-induced communication delay," *IEEE Access*, vol. 5, pp. 27242–27253, 2017.
[21] J. Cai, J. Wan, H. Que, Q. Zhou, and L. Shen, "Adaptive actuator failure compensation control of second-order nonlinear systems with unknown time delay," *IEEE Access*, vol. 6, pp. 15170–15177, 2018.
[22] M.-C. Pai, "Robust tracking and model following for uncertain time-delay systems with input nonlinearity," *Complexity*, vol. 21, no. 2, pp. 66–73, 2015.
[23] H. Zhang, A. Song, and S. Shen, "Adaptive finite-time synchronization control for teleoperation system with varying time delays," *IEEE Access*, vol. 6, pp. 40940–40949, 2018.
[24] W. Zheng, H. Wang, H. Wang, S. Wen, and Z.-M. Zhang, "Fuzzy dynamic output feedback control for T-S fuzzy discrete-time systems with multiple time-varying delays and unmatched disturbances," *IEEE Access*, vol. 6, pp. 31037–31049, 2018.
[25] M. Khazaee, A. H. D. Markazi, and E. Omidi, "Adaptive fuzzy predictive sliding control of uncertain nonlinear systems with bound-known input delay," *ISA Trans.*, vol. 59, pp. 314–324, Nov. 2015.
[26] Q. Zhang, R. Li, and J. Ren, "Robust adaptive sliding mode observer design for T-S fuzzy descriptor systems with time varying delay," *IEEE Access*, vol. 6, pp. 46002–46018, 2018.

[27] B. Xu, Z. Shi, F. Sun, and W. He, "Barrier Lyapunov function based learning control of hypersonic flight vehicle with AOA constraint and actuator faults," *IEEE Trans. Cybern.*, vol. 49, no. 3, pp. 1047–1057, Mar. 2019.

[28] B. Xu, Y. Shou, J. Luo, H. Pu, and Z. Shi, "Neural learning control of strict-feedback systems using disturbance observer," *IEEE Trans. Neural Netw. Learn. Syst.*, vol. 30, no. 5, pp. 1296–1307, May 2019.

[29] T. Teng and R. P. Grant, "Adaptive smith predictor for teleoperation of UAVs using parameter estimation techniques," in *Proc. AIAA SciTech Forum*, CA, USA, Jan. 2019, pp. 1–24.

[30] K.-D. Nguyen, "A predictor-based model reference adaptive controller for time-delay systems," *IEEE Trans. Autom. Control*, vol. 63, no. 12, pp. 4375–4382, Dec. 2018.

[31] A. Benamor and H. Messaoud, "Robust adaptive sliding mode control for uncertain systems with unknown time-varying delay input," *ISA Trans.*, vol. 79, pp. 1–12, Aug. 2018.

[32] M.-C. Pai, "RBF-based discrete sliding mode control for robust tracking of uncertain time-delay systems with input nonlinearity," *Complexity*, vol. 21, no. 6, pp. 194–201, 2016.

[33] Y. Zhang, S. Xie, L. Zhang, and L. Ren, "Robust sliding mode predictive control of uncertain networked control system with random time delay," *Discrete Dyn. Nature Soc.*, vol. 2018, Jul. 2018, Art. no. 6959250.

[34] K. Razi, M. J. Yazdanpanah, and S. S. Ghidary, "Nonlinear H_∞ control of a bilateral nonlinear teleoperation system," *IFAC Proc. Vols.*, vol. 41, no. 2, pp. 12727–12732, 2008.

[35] X. Li and L. Jing, "Global sliding mode control for uncertain linear systems with input time-delays," in *Proc. 8th World Congr. Intell. Control Automat.*, Jinan, China, Jul. 2010, pp. 838–842.

[36] H. C. Barragán, L. P. Osuna-Ibarra, A. G. Loukianov, and F. Plestan, "Sliding mode predictive control of linear uncertain systems with delays," *Automatica*, vol. 94, pp. 409–415, Aug. 2018.

[37] M.-C. Pai, "Chaotic sliding mode controllers for uncertain time-delay chaotic systems with input nonlinearity," *Appl. Math. Comput.*, vol. 271, pp. 757–767, Nov. 2015.

[38] A. Thurling and K. Greene, "An improved predictive algorithm for time delay compensation in UAVs," in *Proc. AIAA AFM*, Montreal, QC, Canada, 2001, pp. 1–11.

[39] L. Guo, F. Cardullo, J. Houck, L. Kelley, and T. Wolters "New predictive filters for compensating the transport delay on a flight simulator," in *Proc. AIAA MST*, Island, 2004, p. 5441.

[40] O. Mofid and S. Mobayen, "Adaptive sliding mode control for finite-time stability of quad-rotor UAVs with parametric uncertainties," *ISA Trans.*, vol. 72, pp. 1–14, Jan. 2018.

[41] G. Shen, Y. Xia, D. Ma, and J. Zhang, "Adaptive sliding-mode control for Mars entry trajectory tracking with finite-time convergence," *Int. J. Robust Nonlinear Control*, vol. 29, no. 5, pp. 1249–1264, 2019.

[42] Z. Wang, Z. Chen, Y. Zhang, X. Yu, X. Wang, and B. Liang, "Adaptive finite-time control for bilateral teleoperation systems with jittering time delays," *Int. J. Robust Nonlinear Control*, vol. 29, no. 4, pp. 1007–1030, 2019.

[43] L. Qiao and W. Zhang, "Double-loop integral terminal sliding mode tracking control for UUVs with adaptive dynamic compensation of uncertainties and disturbances," *IEEE J. Ocean. Eng.*, vol. 44, no. 1, pp. 29–53, Jan. 2019.

[44] L. Qiao and W. Zhang, "Adaptive second-order fast nonsingular terminal sliding mode tracking control for fully actuated autonomous underwater vehicles," *IEEE J. Ocean. Eng.*, vol. 44, no. 2, pp. 363–385, Apr. 2019.

[45] A. Sarhan and S. Qin, "Robust adaptive flight controller for UAV systems," in *Proc. 4th Int. Conf. Inf. Sci. Control Eng. (ICISCE)*, Changsha, China, Jul. 2018, pp. 1214–1219.

[46] X. Hu, B. Xu, and C. Hu, "Robust adaptive fuzzy control for HFV with parameter uncertainty and unmodeled dynamics," *IEEE Trans. Ind. Electron.*, vol. 65, no. 11, pp. 8851–8860, Nov. 2018.

[47] M. P. Aghababa and M. E. Akbari, "A chattering-free robust adaptive sliding mode controller for synchronization of two different chaotic systems with unknown uncertainties and external disturbances," *Appl. Math. Comput.*, vol. 218, no. 9, pp. 5757–5768, 2012.

[48] M. M. Ploycarpou and P. A. Ioannou, "A robust adaptive nonlinear control design," *Automatica*, vol. 32, no. 3, pp. 423–427, 1996.

[49] B. Xu and P. Zhang, "Minimal-learning-parameter technique based adaptive neural sliding mode control of MEMS gyroscope," *Complexity*, vol. 2017, Jul. 2017, Art. no. 6019175.

HONGYANG XU received the B.S. degree from the School of Equipment Engineering, Shenyang Ligong University, in 2013, and the M.S. degree from the School of Astronautics, Northwestern Polytechnical University, in 2016, where she is currently pursuing the Ph.D. degree. Her research interests include guidance and control for UAV.

YONGHUA FAN received the B.S. degree in mechanics and control from Second Artillery Engineering University, China, in 1998, and the Ph.D. degree in control theory and engineering from Northwestern Polytechnical University, China, in 2008, where he has been a Professor with the School of Astronautics, since 2012. His research interests include guidance and control for UAV.

QUANCHENG LI received the B.S. and M.S. degrees from the School of Astronautics, Northwestern Polytechnical University, in 2010 and 2013, respectively, where he is currently pursuing the Ph.D. degree. His research interest includes trajectory optimization for hypersonic vehicles.

FAN WANG received the B.S. and M.S. degrees from the School of Astronautics, Northwestern Polytechnical University, in 2017, where she is currently pursuing the Ph.D. degree. Her research interests include guidance and control for the air-breathing hypersonic vehicle.

JIE YAN was born in 1960. He received the Ph.D. degree from the School of Astronautics, Northwestern Polytechnical University, in 1988, where he is currently a Professor and the Ph.D. Candidate Supervisor. His research interests include flight control, guidance, system simulation, and aircraft design.